Cu(I)-catalysed enantioselective chlorine atom transfer with vinyl radicals

Jun-Bin Tang[1,2,4], Jun-Qian Bian[1,2,4], Zhihan Zhang[1,2,4], Yong-Feng Cheng[1,2], Li Qin[1,2], Qiang-Shuai Gu[3] ✉, Peiyuan Yu[1] ✉ & Xin-Yuan Liu[1,2] ✉

[1]Shenzhen Grubbs Institute and Department of Chemistry, Southern University of Science and Technology, Shenzhen 518055, China.

[2]Shenzhen Key Laboratory of Cross-Coupling Reactions, Southern University of Science and Technology, Shenzhen 518055, China

[3]Academy for Advanced Interdisciplinary Studies and Department of Chemistry, Southern University of Science and Technology, Shenzhen 518055, China.

✉email: guqs@sustech.edu.cn; yupy@sustech.edu.cn; liuxy3@sustech.edu.cn

Abstract: Enantioselective intermolecular atom transfer reactions of vinyl radicals have hitherto remained elusive mainly due to their inherently high instability and reactivity which significantly compromises the stereodiscriminating substrate-catalyst interactions. Herein, we describe Cu(I)-catalyzed enantioselective chlorine atom transfer with vinyl radicals using tailormade tridentate anionic *N,N,N*-ligands featuring bulky peripheral substituents. This reaction readily accommodates (hetero)aryl and alkyl sulfonyl chlorides as radical precursors and more importantly, a large panel of 2-aminoaryl and 2-oxyaryl alkynes as substrates, providing highly transformable axially chiral vinyl chlorides in moderate to good yield with excellent enantioselectivity. The reaction can be easily scaled up to gram scales and straightforward manipulations of the thus obtained vinyl halides lead to axially chiral thiourea, pyridyl carboxamide, and quinolyl sulfonamide compounds, which are promising chiral reagents for asymmetric catalysis. Both experimental and theoretical mechanistic studies supported the proposed chlorine atom transfer reaction mechanism.

Main Text:

Atom transfer, one of the prototypical and important elementary radical reactions[1], is involved in many useful radical transformations such as atom transfer radical addition/polymerization[2–5], which has found numerous applications in organic synthesis and medicinal and material sciences (Fig. 1a). Despite the recent enormous development of radical asymmetric catalysis[6–20], investigations of chemocatalytic enantioselective atom transfer reactions have only met with limited success using chiral Lewis acid catalysis[21,22], organocatalysis[23,24], or transition metal catalysis[6,9,10,25–30]. Of particular note is the incompatibility of almost all these chiral catalytic systems with vinyl radical species in spite of their excellent and well-investigated reactivity towards hydrogen[31,32], halogen[33,34], and chalcogen[35] atom transfer. The major challenge likely stems from their inherently much higher reactivity (corresponding C–H bond dissociation energy (BDE): ~98–110 kcal/mol[36]) than most alkyl radicals (corresponding C–H BDE: <90 kcal/mol[36]) that have been successfully accommodated[16,17], which renders the stereochemical control more difficult.

In this regard, radical addition to alkynes provides convenient access to vinyl radicals since direct single electron reduction of vinyl halides is much more difficult than that of their alkyl counterparts[37]. Thus, a number of non-enantioselective radical alkyne functionalization methodologies[38–40], particularly those under transition metal catalysis[41–44], have been developed for the rapid and convenient access to structurally complex and diverse molecules given the ready availability of both alkynes and various radical precursors and the usually robust radical alkyne addition[39]. Nonetheless, enantioselective versions of these reactions have only sparsely been achieved[45–48] and none of them have so far allowed for the realization of enantioselective intermolecular atom transfer reactions with vinyl radicals and thus, the development of a novel catalytic system is highly desirable and in great demand.

Our group has long been investigating asymmetric radical reactions using chiral copper catalysis[49–54]. Especially, we have recently disclosed the development of tailormade *N*,*N*,*N*-ligands for copper-catalyzed enantioselective alkynyl-group transfer by tertiary alkyl radicals[55]. Long-spreading side arms are deliberately introduced to these ligands to elicit highly efficient stereodiscrimination of motifs in tertiary radicals, which are remote away from the copper center in the key enantioselective homolytic radical substitution-type C–C bond coupling. These results prompted us to investigate whether this strategy would be generally applicable to transition metal-catalyzed atom transfer reactions, particularly, with the highly reactive vinyl radicals (Fig. 1b). To this end, we first envisioned that radical addition to *ortho*-substituted aryl alkynes would generate vinyl radicals and subsequent enantioselective halogen atom transfer[25,26] from chiral metal complexes by these vinyl radicals might provide axially chiral vinyl halides[48,56–82]. In this scenario, the use of copper catalysts seemed to be privileged since copper(II) halides are reported to undergo fast halogen atom transfer (XAT), which would efficiently suppress the non-stereoselective background XAT of vinyl radicals with organohalide starting materials[83]. More importantly, we speculated that appropriate peripheral ligand modifications would be indispensable for achieving competent stereodiscrimination of the *ortho*-substituents on the aryl rings which are far away from the copper centers[55]. Notably, chiral organohalides are well-established robust intermediates with numerous synthetic applications[84,85], particularly in transition-metal catalyzed cross-coupling reactions[84], and thus, the enantioselective synthesis of vinyl halides[70,86–93], if successfully achieved, would provide a versatile synthetic hub for a diverse range of axially chiral alkene compounds[48,62–78,80–82]. Herein we report our efforts in developing the copper-catalyzed enantioselective chlorine atom transfer with vinyl radicals, thus providing axially chiral vinyl chlorides from a broad range of aryl alkynes and diverse sulfonyl chlorides[94–96] with high enantioselectivity (Fig. 1c). The synthetic potential of this reaction was demonstrated by $C(sp^2)$–$C(sp/sp^2)$ cross-coupling of these vinyl chloride products followed by other straightforward

manipulations, leading to promising axially chiral alkene reagents for asymmetric catalysis. Our experimental and theoretical mechanistic results supported the radical mechanism, particularly the XAT step, of the reaction.

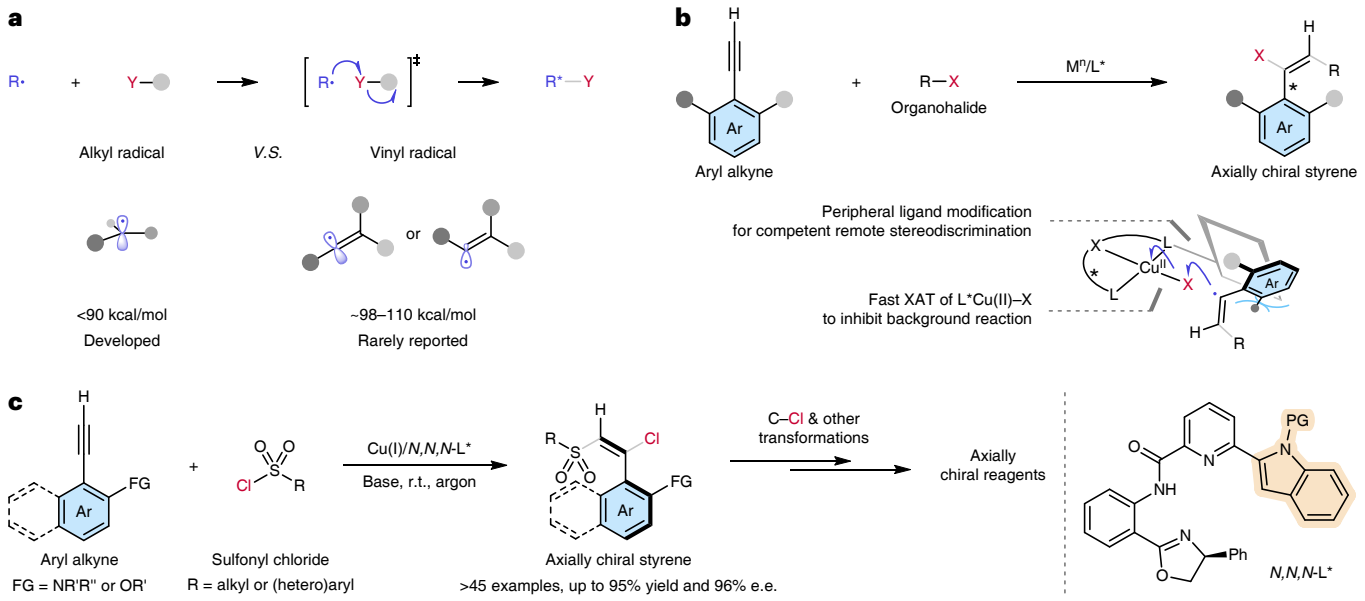

Fig. 1 | Motivation and design of Cu(I)-catalysed enantioselective chlorine atom transfer by vinyl radicals. a, The enantioselective atom transfer reactions have been developed for only relatively stable alkyl radicals (corresponding C–H BDE: <90 kcal/mol) while that for more reactive vinyl radicals (corresponding C–H BDE: ~98–110 kcal/mol) have hitherto remained rarely reported. **b**, To develop enantioselective halogen atom transfer with vinyl radicals resulting from radical addition to alkynes, we proposed to take advantage of the relatively fast XAT of chiral L*Cu(II)X species to inhibit nonstereoselective background reactions between vinyl radicals and organohalide radical precursors. In addition, we conjectured that appropriate ligand peripheral substituents would be essential for invoking competent stereodiscrimination interactions with remote motifs of vinyl radicals. **c**, We achieved highly enantioselective chlorine atom transfer reaction of sulfonyl chlorides with aryl alkynes by Cu(I) catalysis with tailormade chiral *N,N,N*-ligands. Ar, aryl; XAT, halogen atom transfer; r.t., room temperature; PG, protecting group.

Results and discussion

Reaction development. At the beginning of the investigation, we took 2-aminoaryl alkyne **NS1** as the model starting material given the widely explored use of axially chiral aryl amine compounds[97,98]. An initial screening of ligands employed in our previous works revealed that both oxazoline-based *N*,*N*,*P*-ligand **L2**[99] (entry 2; Table 1) and *N*,*N*,*N*-ligand **L3**[100,101] (entry 3) but the Dixon's *N*,*N*,*P*-ligand **L1**[52,102] (entry 1) afforded low yet significant enantioselectivity. As proposed above, the introduction of a 6-phenyl ring to the pyridine motif of **L3** boosted the e.e. value to 40% (entry 4). Replacing the phenyl ring with a bulkier 9-anthracenyl group greatly enhanced the e.e. value to 77% (entry 5) and further switching to a non-symmetrically bulky 2-indolyl group ultimately gave excellent enantioselectivity (entry 6). Nonetheless, the reaction efficiency was generally low with these tested ligands (entries 1–6) likely due to the steric congestion around the copper center caused by the bulky *tert*-butyl group on the oxazoline ring (see Supplementary Figs. 1 and 2 for X-ray structures of **L6** and **L7**). Accordingly, a phenyl ring in place of this *tert*-butyl group resulted in substantially increased yield with almost unaltered enantioselectivity (entry 7). Additional condition optimizations in terms of copper salts, base additives, and solvents (Supplementary Table 1) revealed the optimal conditions (entry 8) as follows: **NS1** (0.20 mmol) and **S1** (1.5 equiv.) in the presence of $[Cu(MeCN)_4]PF_6$ (10 mol%), **L7** (10 mol%), and K_3PO_4 (3.0 equiv.) in mixed DME/MTBE (v/v 1/3, 4.0 ml) at r.t. for 5 days under argon, giving **N1** in 80% yield with 93% e.e.

Table 1 | Effect of chiral ligands

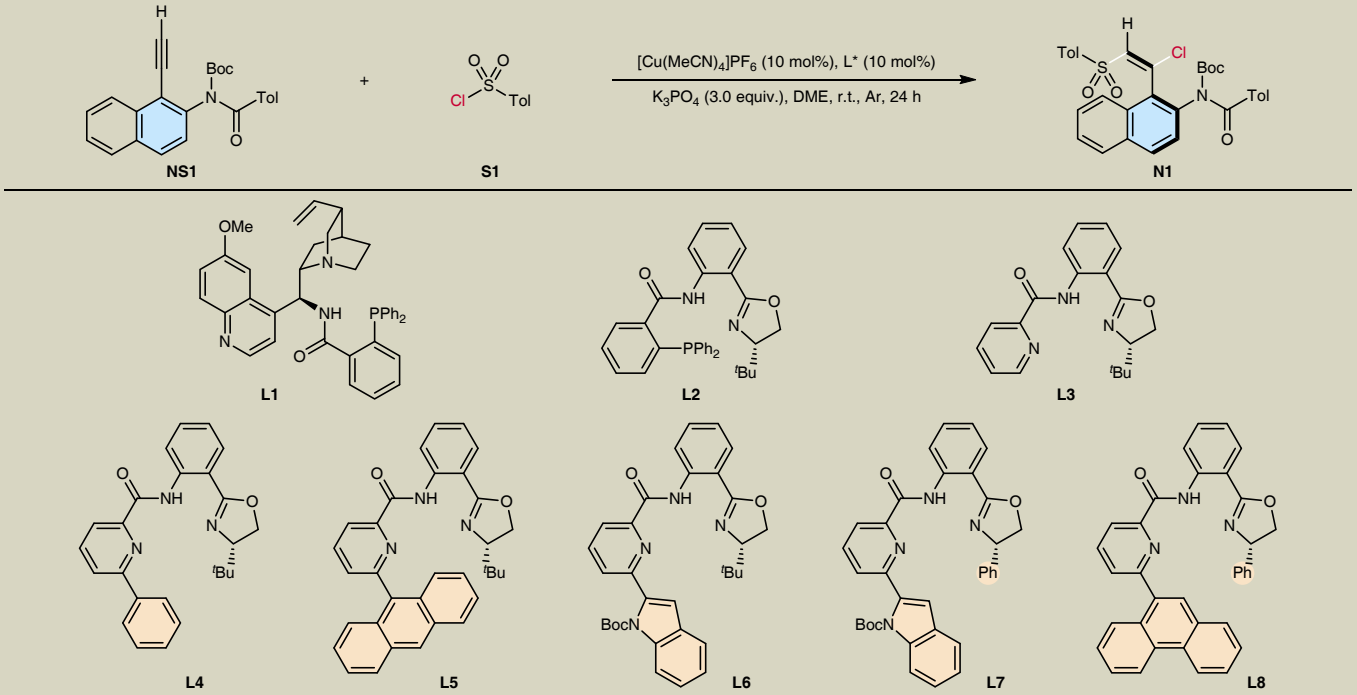

Entry	L*	Yield/%	E.e./%
1	**L1**	10	5
2	**L2**	40	20
3	**L3**	21	28
4	**L4**	35	40
5	**L5**	47	77
6	**L6**	45	93
7	**L7**	68	94
8[a]	**L7**	80	93

Reaction conditions: **NS1** (0.050 mmol, 1.0 equiv.), **S1** (1.5 equiv.), $[Cu(MeCN)_4]PF_6$ (10 mol%), L* (10 mol%), and K_3PO_4 (3.0 equiv.) in DME (1.0 ml) at r.t. for 24 h under argon. Yield of **N1** is based on ^{1}H-NMR analysis of the crude products using dibromomethane as an internal standard; E.e. of **N1** is based on chiral HPLC analysis. [a]**NS1** (0.20 mmol) in DME/MTBE (v/v 1/3, 4.0 mL) for 5 d. Boc, *tert*-butyloxycarbonyl; Tol, *p*-toluenyl; DME, 1, 2-dimethoxyethane; Ar, argon; MTBE, methyl *tert*-butyl ether.

Substrate scope. We first investigated the scope of sulfonyl chlorides and found excellent tolerance of unsubstituted phenyl sulfonyl chlorides and those bearing a wide range of functional groups with different

electronic properties on the *para*-, *meta*-, or *ortho*-position (**N1**–**N12**; Fig. 2). Particularly, reactive halides (**N3**, **N4**, **N9**, and **N10**) and acidic acetamides (**N8**) are well tolerated and nitro (**N6**) and cyano (**N7**) groups which are usually problematic in copper-catalyzed radical transformations are also compatible with this reaction. In addition, 2-thiophenyl (**N13**) and 3-pyridyl (**N14**) substituted heteroaryl sulfonyl chlorides are applicable to this transformation. Notably, primary (**N15**) and secondary (**N16**–**N18**) alkyl sulfonyl chlorides are viable radical precursors for this reaction. As for the scope of 2-aminoaryl alkynes, a series of 6-substituted naphthyl rings (**N19**–**N22**) are readily accommodated in this reaction while a 7-methoxyl group (**N23**) leads to greatly diminished enantioselectivity. By contrast, a panel of 5- and/or 6-substituted phenyl rings all are suitable for this reaction, providing **N24**–**N28** in good yield with excellent enantioselectivity. Regarding the 2-amino group, both two imide substrates (**N1** and **N29**; see Supplementary Table 2 for condition optimizations of **N29**) delivered higher enantioselectivity than an amide one (**N30**; see Supplementary Table 3 for condition optimizations), which in turn performed better than a urea substrate (**N31**).

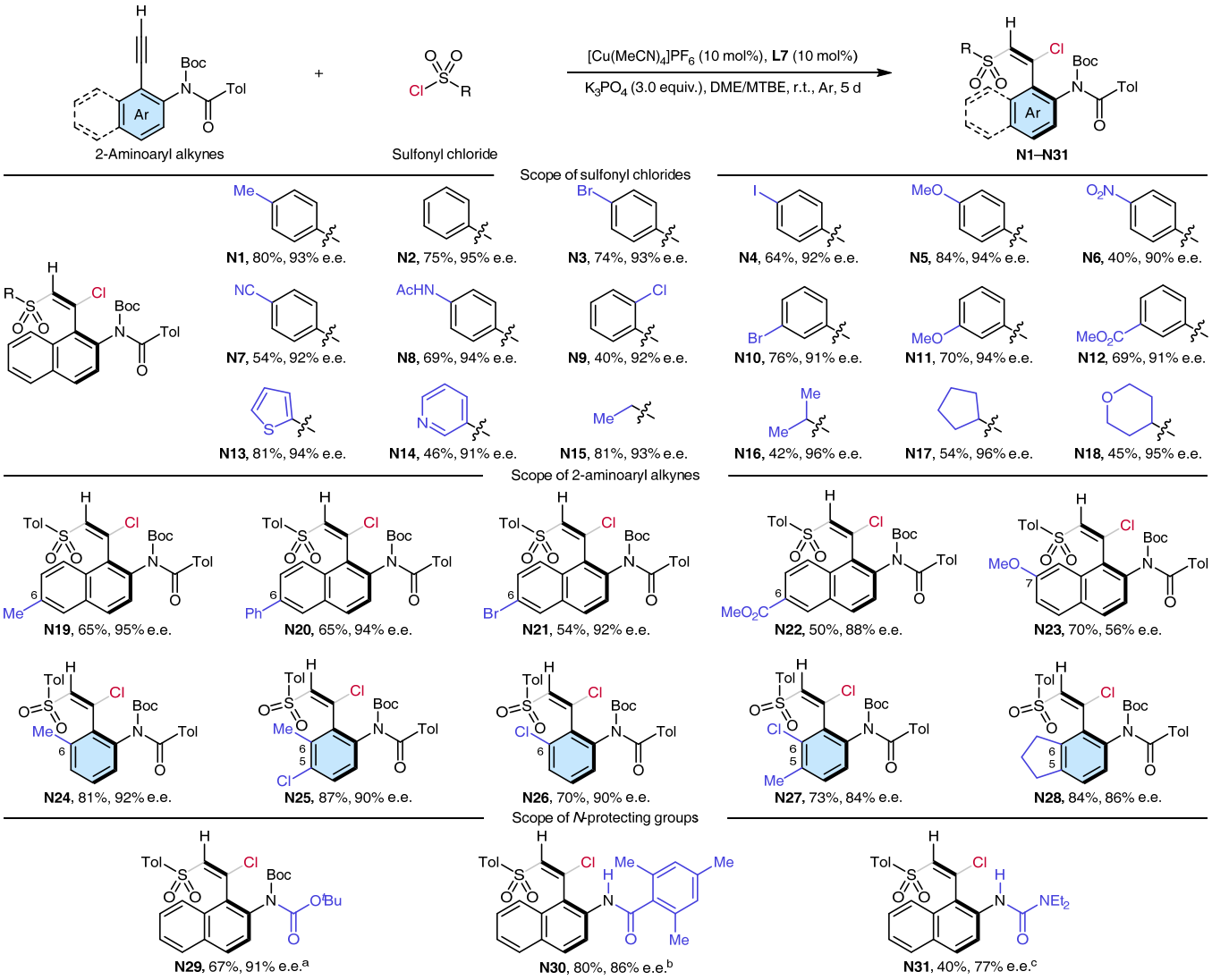

Fig. 2 | Substrate scope for sulfonyl chlorides and 2-aminoaryl alkynes. Standard reaction conditions: 2-aminoaryl alkyne (0.20 mmol, 1.0 equiv.), sulfonyl chloride (1.5 equiv.), $[Cu(MeCN)_4]PF_6$ (10 mol%), **L7** (10 mol%), and K_3PO_4 (3.0 equiv.) in DME/MTBE (v/v = 1/3, 4.0 ml) at r.t. for 5 d under argon. Isolated yields are shown; E.e. is based on chiral HPLC analysis. [a]CuCl (10 mol%), 2-(diphenylphosphaneyl)pyridine (10 mol%), and **L8** (10 mol%) in THF (4.0 ml) at 0 °C. [b]**L6** (10 mol%) in DCM/toluene (v/v = 1/3, 4.0 ml) at −10 °C. [c]**L6** (10 mol%) in DCM (4.0 ml). Ac, acetyl; THF, tetrahydrofuran; DCM, dichloromethane.

Considering the high utility of axially chiral phenol compounds[97,98], we next investigated the reaction with 2-oxyaryl alkynes. Fortunately, excellent enantioselectivity of product **O1** was observed under the aforementioned optimal conditions albeit with only low yield (46% yield, 92% e.e.; Supplementary Table 4). These results encouraged us to further examine the effects of ligands, solvents, and copper sources, during which a straightforward solvent change to ethyl acetate led to not only high reaction efficiency but also outstanding enantioselectivity (90% yield; 92% e.e.; Supplementary Table 4). Accordingly, we next explored the scope of 2-oxyaryl alkynes and found a range of naphthyl rings without or with additional substituents at 4- and 6-positions were well tolerated (**O1**–**O10**, Fig. 3). In accord with the results of 2-aminoaryl alkynes (Fig. 2), the 7-substitution of 2-oxyaryl substrates also resulted in greatly decreased enantioselectivity (**O11**). Likewise, good tolerance of 5- and/or 6-substitution of 2-oxyphenyl alkyne substrates was also observed (**O12** and **O13**). In addition, 4,6-disubstituted 2-oxyphenyl alkynes were applicable, too, to this reaction, affording good enantioselectivity with high yield (**O14**). As for the 2-oxy functionality, carbamate (e.g., **O1**) and carbonate (**O15**; see Supplementary Table 5 for condition optimizations), as well as carboxylic (**O16**) and sulfonyl ester (**O17**), groups proved to be workable in this reaction, providing the desired products in high enantioselectivity with varied yield. The absolute structures of products **N1** (Supplementary Fig. 3), **N30** (Supplementary Fig. 4), and **O1** (Supplementary Fig. 5) all were determined to be *R*a by X-ray structural analysis and those of other products were assigned by analogy.

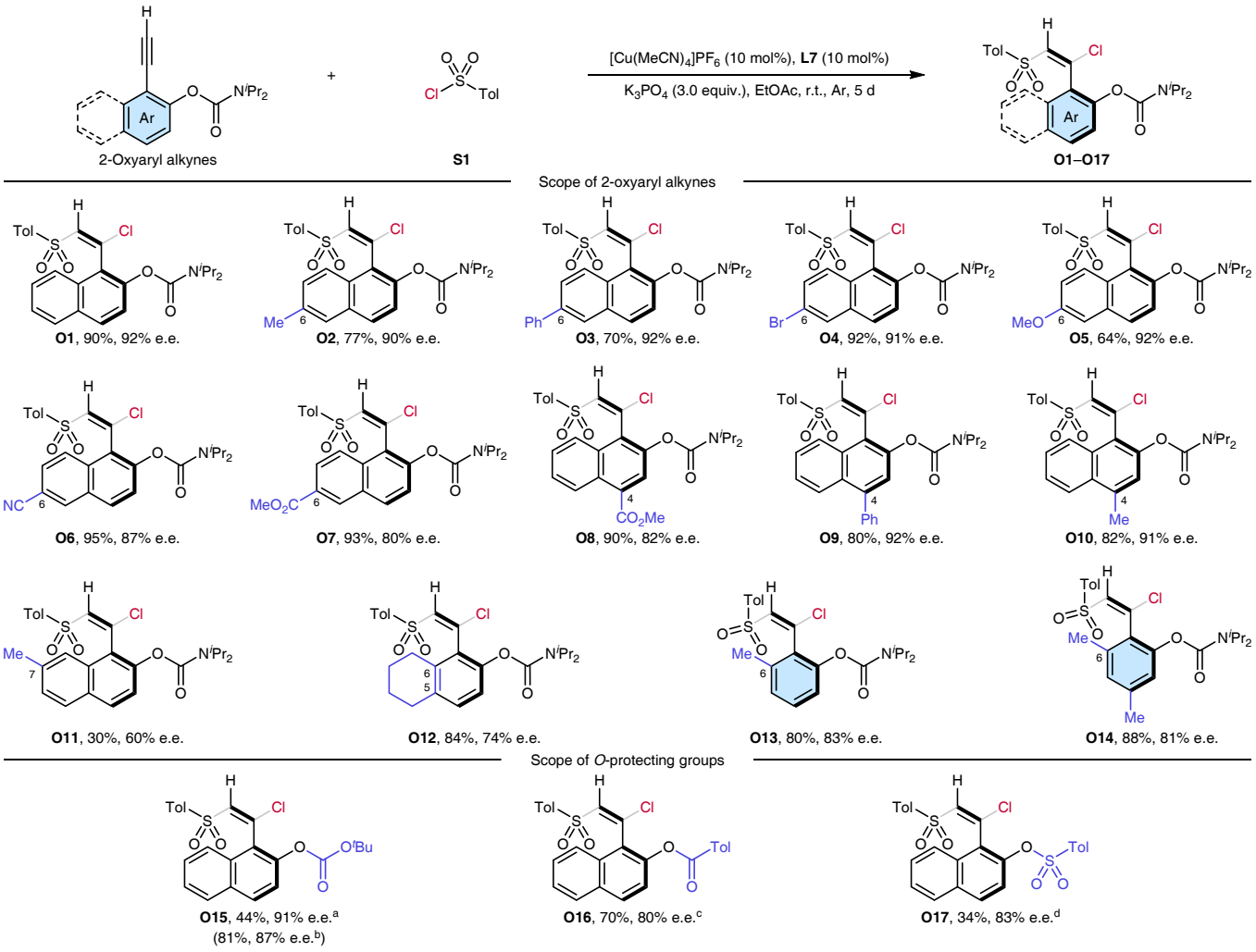

Fig. 3 | Substrate scope for 2-oxyaryl alkynes. Standard reaction conditions: 2-oxyaryl alkyne (0.20 mmol, 1.0 equiv.), **S1** (1.5 equiv.), $[Cu(MeCN)_4]PF_6$ (10 mol%), **L7** (10 mol%), and K_3PO_4 (3.0 equiv.) in EtOAc (4.0 ml) at r.t. for 5 d under argon. Isolated yields are shown; E.e. is based on chiral HPLC analysis. [a]2-(Diphenylphosphaneyl)pyridine (10 mol%) and **L6** (10 mol%) in DME (4.0 ml) at 0 °C. [b]**L6** (10 mol%) in DME (4.0 ml). [c]**L6** (10 mol%). [d]**L6** (10 mol%) at 0 °C.

Synthetic utility. To demonstrate the synthetic potential of these axially chiral vinyl chloride products, we first carried out gram-scale reactions of both 2-aminoaryl and 2-oxyaryl alkyne substrates **NS1** (Fig. 4a)

and **OS1** (Fig. 4b) and still obtained good yield with excellent enantioselectivity. Next, we examined their thermal stability and observed marginal racemization up to 60 °C (Figs. 4c and 4d; see Supplementary Tables 6 and 7 for more details). Accordingly, we managed to perform Sonogashira and Suzuki–Miyaura coupling reactions with these axially chiral vinyl chlorides at or below 60 °C, which generally yielded the corresponding products with highly retained enantiopurity (Fig. 4e). In addition, subsequent straightforward deprotection and *N*-functionalization gave rise to axially chiral thiourea **N1-4**, pyridinyl carboxamide **N1-5**, and quinolyl sulfonamide **N1-6** (Fig. 4f), which are promising hydrogen bonding catalysts[103–105] or *N*,*N*-bidentate ligands[50]. Notably, the stereointegrity was generally maintained throughout the manipulation processes, thus showcasing the high utility and versatility of our reaction as a competent synthetic hub in preparing axially chiral alkene reagents for asymmetric catalysis and synthesis.

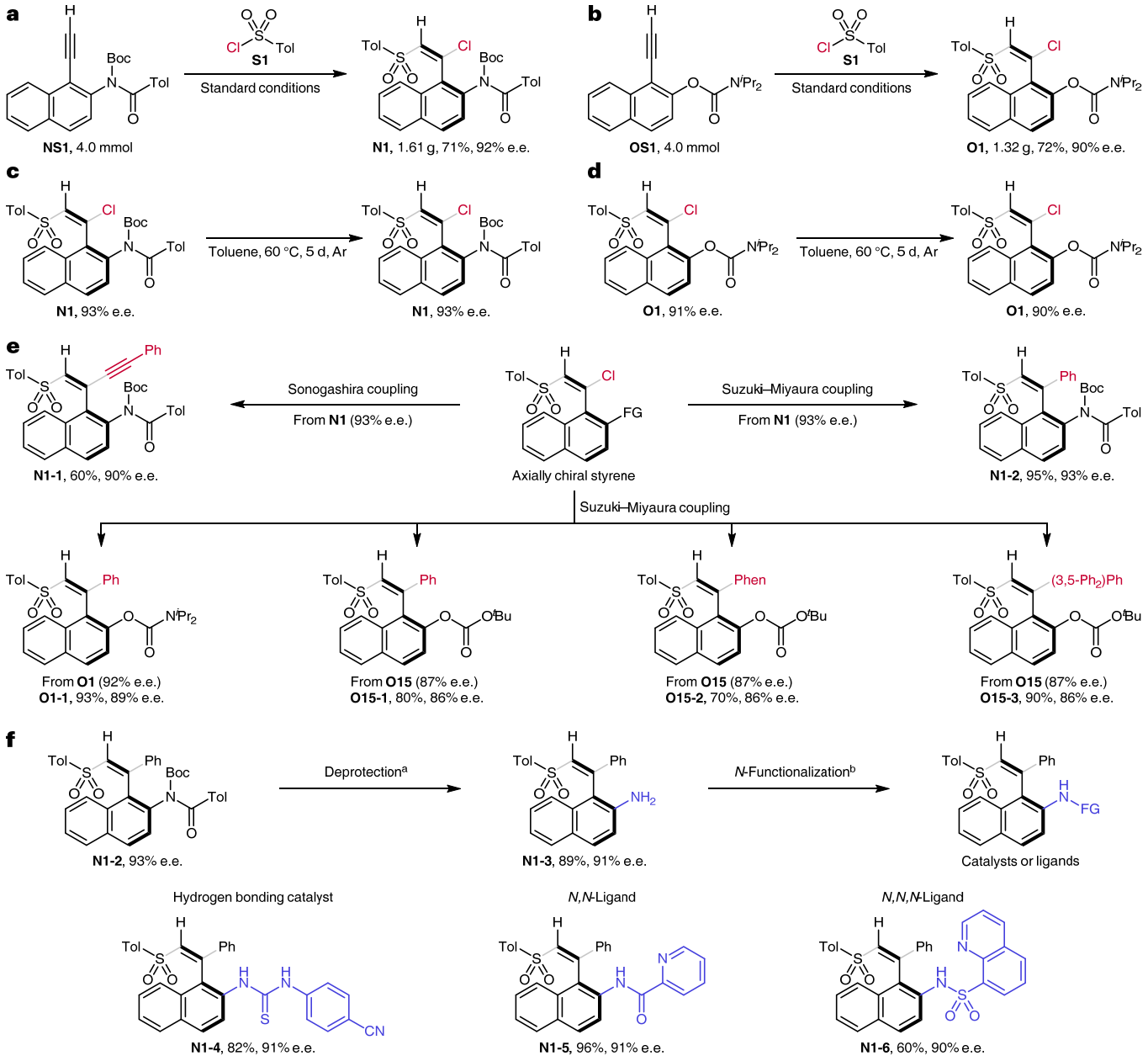

Fig. 4 | Synthetic utility for the construction of valuable axially chiral reagents. a and **b**, The reactions were readily scaled up to gram scales. **c** and **d**, The thus-obtained axially chiral products displayed robust thermostability at up to 60 °C in terms of enantiopurity. **e**, The axially chiral vinyl chloride products readily participated in Sonogashira and Suzuki–Miyaura C–C bond coupling reactions without any significant loss of enantiopurity. **f**, The amino groups in the thus-obtained products were smoothly deprotected and

functionalized afterwards, providing potentially valuable axially chiral hydrogen bonding catalysts and ligands. Phen, 9-phenanthryl. [a]Conditions: i) K_2CO_3, EtOH, 60 °C, Ar, 48 h; ii) TFA/DCM (v/v = 1/1), r.t., Ar, 12 h. [b]Conditions for **N1-4**: 4-isothiocyanatobenzonitrile, DMAP, DCM, r.t., Ar, 48 h; For **N1-5**: picolinic acid, DMAP, DCC, DCM, r.t., Ar, 24 h; For **N1-6**: quinoline-8-sulfonyl chloride, DMAP, pyridine, DCM, 50 °C, Ar, 3 d. Phen, 9-phenanthryl; TFA, trifluoroacetic acid; DMAP, 4-dimethylaminopyridine; DCC, *N*,*N*′-dicyclohexylcarbodiimide.

Mechanistic considerations. Control experiments in the absence of the copper salt, chiral ligand, or base additive confirmed that all of them were indispensable for the reaction (Supplementary Tables 8 and 9). In the presence of either TEMPO ((2,2,6,6-tetramethylpiperidin-1-yl)oxyl; Supplementary Tables 8 and 9) or BHT (butylated hydroxytoluene; Fig. 5a and Supplementary Table 10), the reaction was remarkably retarded with decreased yield and enantioselectivity. In addition, sulfonyl radical-trapped products **BHT-Ts1** and **BHT-Ts2** were isolated in the reaction with BHT (Fig. 5a and Supplementary Table 10). These results supported the proposed radical mechanism that involves sulfonyl radicals. Interestingly, the reaction with the 1,6-bis-alkyne substrate **OS18** predominantly occurred at the apparently more hindered 1-alkyne position (Fig. 5b). Thus, the corresponding singly functionalized product **O18** was favorably formed in high enantioselectivity together with a trace amount of doubly functionalized product **O18''** while the other possible singly functionalized product **O18'** was not observed. By contrast, all these products were obtained in roughly comparable yield under photochemical conditions. These results possibly indicated the participation of the copper catalyst in the radical alkyne addition step, which actively adjusted the regioselectivity.

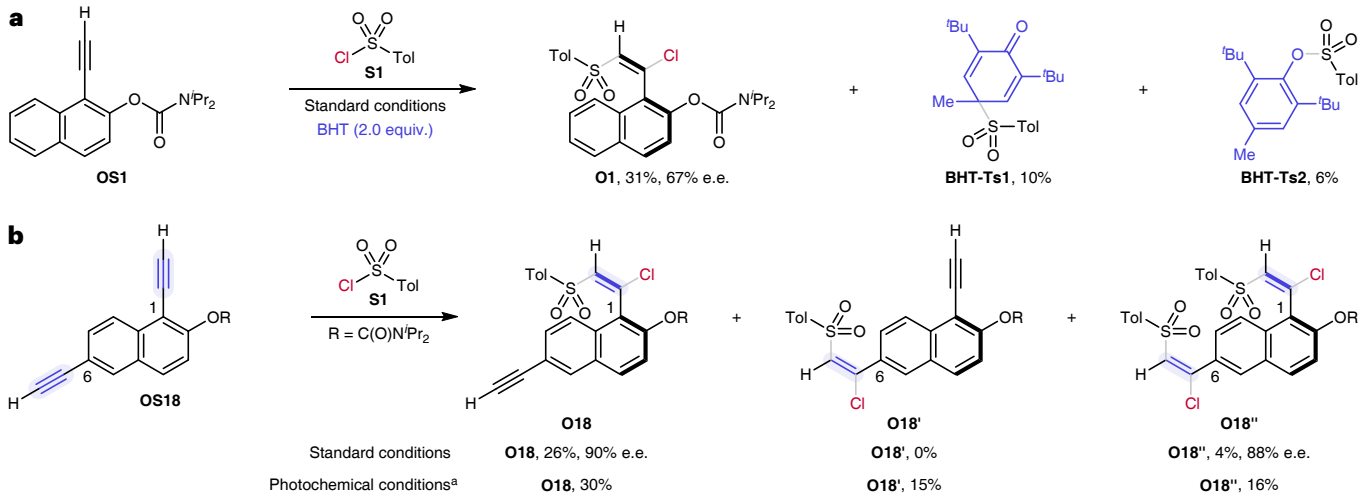

Fig. 5 | Mechanistic experiments. a, The reaction was inhibited by BHT and provided sulfonyl radical-trapped products, supporting a radical reaction mechanism. **b**, The reaction of bis-alkynyl substrate **OS18** yielded **O18** as the predominant regioisomer under the standard reaction conditions while that under photochemical conditions gave all possible regioisomers in comparable yield. These results possibly suggested the involvement of copper catalyst in the radical addition step. [a][Cu(MeCN)$_4$]BF$_4$ (5.0 mol%), 2,9-dimethylphenanthroline (10 mol%), blue LED (450 nm), $CHCl_3$, r.t., Ar, 4 d. BHT, 2,6-di-*tert*-butyl-4-methylphenol.

Density functional theory (DFT) calculations with deprotonated anionic **L7** as a model ligand were next used to explore the reaction mechanisms of the radical transformation and the origin of the enantioselective construction of axially chiral vinyl chlorides. As shown in Fig. 6a, the S–Cl bond of *p*-TsCl (**S1**) is homolytically cleaved to generate sulfonyl radical and Cu(II)Cl complex **IM1** through a chlorine atom abstraction transition state ($\mathbf{TS_{ClAA}}$) mediated by Cu(I) complex **CAT**. The calculated spin density of $\mathbf{TS_{ClAA}}$ clearly features an open shell singlet state where the alpha electron localizing on Cu antiferromagnetically couples with the beta electron localizing on sulfonyl radical. This sulfonyl radical further undergoes radical addition with alkyne under the chiral environment of Cu(II)Cl complex **IM1**

through $\mathbf{TS_{RA\text{-}Cu\text{-}}}_{\boldsymbol{f}}$ and $\mathbf{TS_{RA\text{-}Cu\text{-}}}_{\boldsymbol{dis}}$, affording the sulfonyl vinyl radical in either *R* or *S* configuration, respectively. These asymmetric sulfonyl vinyl radicals are easily captured by Cu(II)Cl complex **IM1** via $\mathbf{TS_{ClAT\text{-}}}_{\boldsymbol{f}}$ and $\mathbf{TS_{ClAT\text{-}}}_{\boldsymbol{dis}}$ with energy barriers less than 12 kcal/mol, resulting in the chlorinated atropisomers of **O1** with the regeneration of Cu(I) complex **CAT**. The inner-sphere mechanism involving a Cu(III) intermediate has been examined to be disfavored as the energy barrier required for the reductive elimination step is much larger than that of the Cl atom transfer step (see Supplementary Fig. 6). Interestingly, the transition state of free radical addition ($\mathbf{TS_{RA}}$) of sulfonyl radical to alkyne without the involvement of a Cu(II) complex lies much higher in energy due to the absence of non-covalent interactions between the alkyne substrate and the ligand. This free radical addition could only afford vinyl radicals in both configurations without any enantio-differentiation (see Supplementary Fig. 7). The rotation barrier of this vinyl radical along the axial C–C bond was calculated to be higher than the forward Cl atom transfer process (see Supplementary Fig. 8). This indicates that the interconversion between the two desymmetrized radicals is not fast enough and thus, the chlorination is irreversible. The radical addition involving **IM1** results in good enantioselectivity due to the chiral environment defined by the chiral ligand. This is consistent with the mechanistic experiments that suggest the possible involvement of the Cu complex in the radical addition step (Fig. 5b). The difference in energy barriers between the two paths with different configurations ($\Delta\Delta G^{\ddagger}$) was calculated to be 2.2 kcal/mol under the Curtin-Hammett principle, in good accordance with the experimentally observed excellent stereoselectivity. In the favored pathway, the radical capture transition state $\mathbf{TS_{ClAT\text{-}}}_{\boldsymbol{f}}$ is slightly more stable than the previous radical addition transition state $\mathbf{TS_{RA\text{-}Cu\text{-}}}_{\boldsymbol{f}}$, while in the disfavored pathway, the transition states of these two processes are close in energy. Since the stereoelectronic structures of these two Cu(II)-involved radical addition transition states are more comparable and the energy trend retains during the course of chirality induction, the geometries between $\mathbf{TS_{RA\text{-}\ Cu\text{-}}}_{\boldsymbol{f}}$ and $\mathbf{TS_{RA\text{-}Cu\text{-}}}_{\boldsymbol{dis}}$ were carefully examined to rationalize the origin of enantioselectivity (Fig. 6b).

For both transition states, the naphthalene group of **OS1** sustains the non-covalent interactions with the ligand. However, in $\mathbf{TS_{RA\text{-}Cu\text{-}}}\boldsymbol{dis}$, the N^iPr_2 group encounters steric clashes with the backbone phenyl ring of the ligand, while in $\mathbf{TS_{RA\text{-}Cu\text{-}}}\boldsymbol{f}$, the N^iPr_2 group points toward less congested space to avoid this repulsion. Therefore, the **L7Cu** complex provides a chiral environment for both the radical addition and Cl atom transfer steps, which ensures efficient enantio-discrimination.

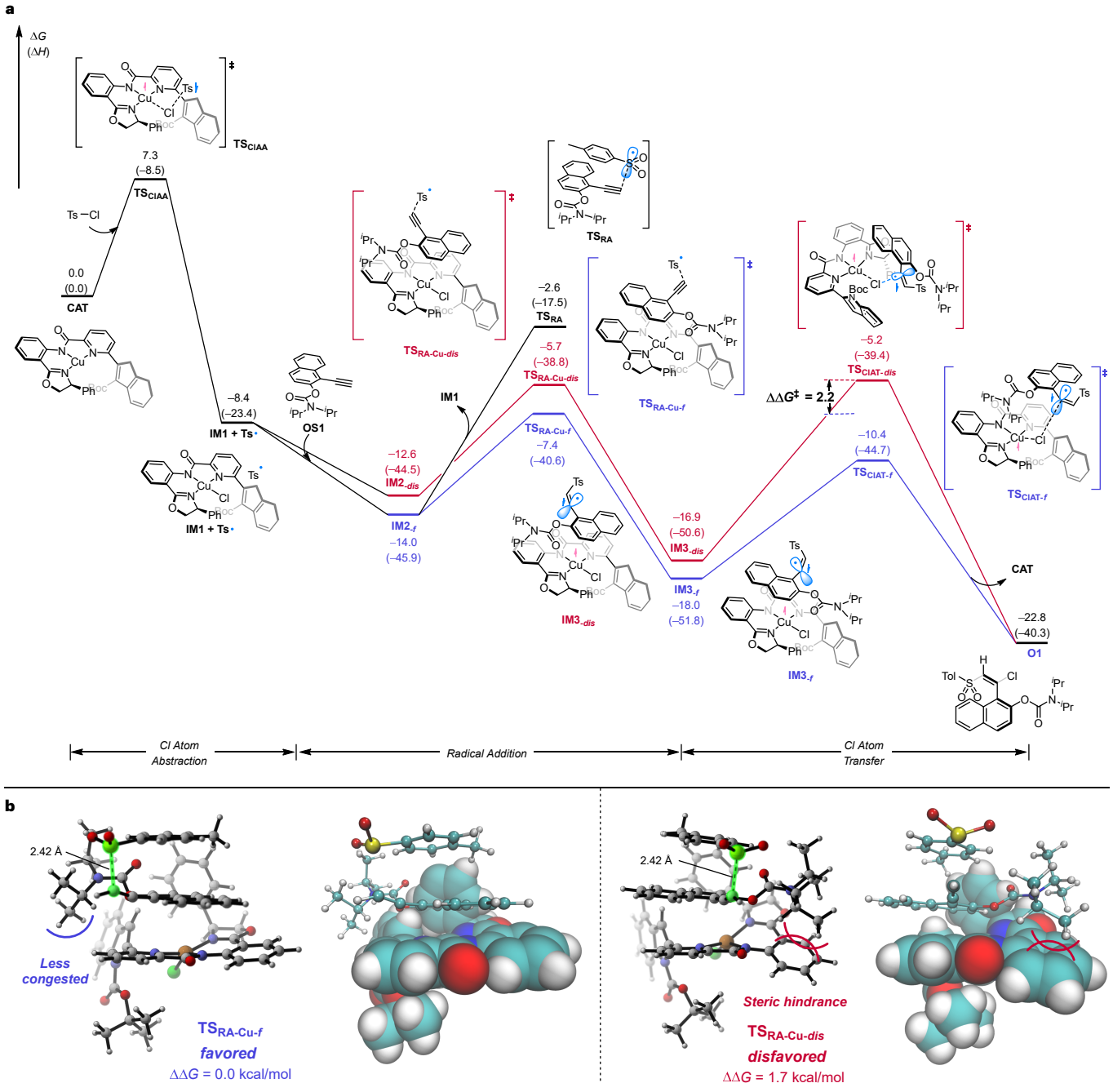

Fig. 6 | Computational studies. a, Energy profiles on the operative catalytic cycle with **L7** used as ligand. The relative free energies and enthalpies (in parentheses) calculated at the (U)wB97XD/PCM/def2TZVP(Cu)-6-311+G(d,p)//(U)B3LYP-D3(BJ)/def2TZVP(Cu)-6-31G(d) level of theory are given in kcal/mol. The catalytic cycle is composed of Cl atom transfer, Cu-involved radical addition to alkyne, and Cl atom transfer to vinyl radical. All transition states except for $\mathbf{TS_{RA}}$ presented on

this energy profile feature open-shell singlet electronic configuration. **b**, 3D structures of key Cu-involved radical addition transition state $\mathbf{TS_{RA\text{-}Cu\text{-}}}\boldsymbol{f}$ and $\mathbf{TS_{RA\text{-}Cu\text{-}}}\boldsymbol{dis}$.

Summary

In sum, we have successfully tailored tridentate anionic *N,N,N*-ligands to realize highly enantioselective chlorine atom transfer with very reactive vinyl radicals under copper catalysis. The installation of sterically bulky groups to the peripheral positions of these *N,N,N*-ligands to elicit competent stereodiscrimination of remote motifs of the vinyl radicals experimentally proves to be essential for attaining high enantioselectivity. The reaction readily affords an abundance of valuable enantioenriched vinyl chlorides, thus providing a robust platform for expedient access to a myriad of axially chiral acyclic styrene compounds with highly promising applications in asymmetric catalysis. These results highlight the great potential of strategically devised multidentate anionic ligands for the development of asymmetric radical reactions of highly reactive carbon radicals using transition metal catalysis, particularly copper catalysis.

References

1. Sherburn, M. S. Basic concepts on radical chain reactions. In *Encyclopedia of Radicals in Chemistry, Biology and Materials* (eds Chatgilialoglu, C. & Studer, A.) (Wiley, 2012).
2. Pintauer, T. & Matyjaszewski, K. Atom transfer radical polymerization (ATRP) and addition (ATRA) and applications. In *Encyclopedia of Radicals in Chemistry, Biology and Materials* (eds Chatgilialoglu, C. & Studer, A.) (Wiley, 2012).
3. Muñoz-Molina, J. M. & Belderrain, T. R. in *C-1 Building Blocks in Organic Synthesis 2 Science of Synthesis* (ed. van Leeuwen, P. W. N. M.) 459–473 (Thieme, Stuttgart, 2014).

4. Matyjaszewski, K. Advanced materials by atom transfer radical polymerization. *Adv. Mater.* **30**, 1706441 (2018).

5. Engl, S. & Reiser, O. Copper-photocatalyzed ATRA reactions: concepts, applications, and opportunities. *Chem. Soc. Rev.* **51**, 5287–5299 (2022).

6. Wang, X. & Zhang, X. P. Catalytic radical approach for selective carbene transfers via cobalt(II)-based metalloradical catalysis. In *Transition Metal-Catalyzed Carbene Transformations* (eds Wang, J., Che, C.-M., & Doyle, M. P.) 25–66 (Wiley, 2022).

7. Xiong, T. & Zhang, Q. Recent advances in the direct construction of enantioenriched stereocenters through addition of radicals to internal alkenes. *Chem. Soc. Rev.* **50**, 8857–8873 (2021).

8. Yin, Y., Zhao, X., Qiao, B. & Jiang, Z. Cooperative photoredox and chiral hydrogen-bonding catalysis. *Org. Chem. Front.* **7**, 1283–1296 (2020).

9. Liu, Y. et al. Iron- and cobalt-catalyzed C(sp^3)–H bond functionalization reactions and their application in organic synthesis. *Chem. Soc. Rev.* **49**, 5310–5358 (2020).

10. Milan, M., Bietti, M. & Costas, M. Enantioselective aliphatic C–H bond oxidation catalyzed by bioinspired complexes. *Chem. Commun.* **54**, 9559–9570 (2018).

11. Zhang, Z., Chen, P. & Liu, G. Copper-catalyzed radical relay in C(sp^3)–H functionalization. *Chem. Soc. Rev.* **51**, 1640–1658 (2022).

12. Lipp, A., Badir, S. O. & Molander, G. A. Stereoinduction in metallaphotoredox catalysis. *Angew. Chem., Int. Ed.* **60**, 1714–1726 (2021).

13. Choi, J. & Fu, G. C. Transition metal–catalyzed alkyl-alkyl bond formation: another dimension in cross-coupling chemistry. *Science* **356**, eaaf7230 (2017).

14. Cherney, A. H., Kadunce, N. T. & Reisman, S. E. Enantioselective and enantiospecific transition-metal-catalyzed cross-coupling reactions of organometallic reagents to construct C–C bonds. *Chem. Rev.* **115**, 9587–9652 (2015).

15. Proctor, R. S. J., Colgan, A. C. & Phipps, R. J. Exploiting attractive non-covalent interactions for the enantioselective catalysis of reactions involving radical intermediates. *Nat. Chem.* **12**, 990–1004 (2020).

16. Sibi, M. P., Manyem, S. & Zimmerman, J. Enantioselective radical processes. *Chem. Rev.* **103**, 3263–3296 (2003).

17. Mondal, S. et al. Enantioselective radical reactions using chiral catalysts. *Chem. Rev.* **122**, 5842–5976 (2022).

18. Zhang, C., Li, Z.-L., Gu, Q.-S. & Liu, X.-Y. Catalytic enantioselective C(sp^3)–H functionalization involving radical intermediates. *Nat. Commun.* **12**, 475 (2021).

19. Silvi, M. & Melchiorre, P. Enhancing the potential of enantioselective organocatalysis with light. *Nature* **554**, 41–49 (2018).

20. Huang, X. & Meggers, E. Asymmetric photocatalysis with bis-cyclometalated rhodium complexes. *Acc. Chem. Res.* **52**, 833–847 (2019).

21. Sibi, M. P. & Sausker, J. B. The role of the achiral template in enantioselective transformations. Radical conjugate additions to α-methacrylates followed by hydrogen atom transfer. *J. Am. Chem. Soc.* **124**, 984–991 (2002).

22. Luo, Y. et al. Enantioselective radical hydroacylation of *α,β*-unsaturated carbonyl compounds with aldehydes by triplet excited anthraquinone. *ACS Catal.* **12**, 12984–12992 (2022).

23. Kong, M. et al. Catalytic reductive cross coupling and enantioselective protonation of olefins to construct remote stereocenters for azaarenes. *J. Am. Chem. Soc.* **143**, 4024–4031 (2021).

24. Shi, Q. et al. Visible-light mediated catalytic asymmetric radical deuteration at non-benzylic positions. *Nat. Commun.* **13**, 4453 (2022).

25. Chen, B., Fang, C., Liu, P. & Ready, J. M. Rhodium-catalyzed enantioselective radical addition of CX_4 reagents to olefins. *Angew. Chem., Int. Ed.* **56**, 8780–8784 (2017).

26. Wu, D., Fan, W., Wu, L., Chen, P. & Liu, G. Copper-catalyzed enantioselective radical chlorination of alkenes. *ACS Catal.* **12**, 5284–5291 (2022).

27. Ge, L. et al. Iron-catalysed asymmetric carboazidation of styrenes. *Nat. Catal.* **4**, 28–35 (2021).

28. Wu, L. et al. Anionic bisoxazoline ligands enable copper-catalyzed asymmetric radical azidation of acrylamides. *Angew. Chem., Int. Ed.* **60**, 6997–7001 (2021).

29. Liu, W. et al. Iron-catalyzed enantioselective radical carboazidation and diazidation of *α,β*-unsaturated carbonyl compounds. *J. Am. Chem. Soc.* **143**, 11856–11863 (2021).

30. Xu, P., Xie, J., Wang, D.-S. & Zhang, X. P. Metalloradical approach for concurrent control in intermolecular radical allylic C−H amination. *Nat. Chem.* **15**, 498–507 (2023).

31. Dénès, F., Beaufils, F. & Renaud, P. Preparation of five-membered rings via the translocation-cyclization of vinyl radicals. *Synlett* **2008**, 2389–2399 (2008).

32. Yue, B., Wu, X. & Zhu, C. Recent advances in vinyl radical-mediated hydrogen atom transfer. *Chin. J. Org. Chem.* **42**, 458–470 (2022).

33. Fu, B. et al. Recent advances on the halo- and cyano-trifluoromethylation of alkenes and alkynes. *Molecules* **26**, 7221 (2021).

34. Shi, Z.-Z. et al. Recent advances in radical cascade cyclization of 1,n-enynes with trifluoromethylating agents. *Tetrahedron* **131**, 133216 (2023).

35. Dénès, F., Schiesser, C. H. & Renaud, P. Thiols, thioethers, and related compounds as sources of c-centred radicals. *Chem. Soc. Rev.* **42**, 7900–7942 (2013).

36. Luo, Y.-R. *Comprehensive Handbook of Chemical Bond Energies* (CRC Press, 2007).

37. Pagire, S. K., Föll, T. & Reiser, O. Shining visible light on vinyl halides: expanding the horizons of photocatalysis. *Acc. Chem. Res.* **53**, 782–791 (2020).

38. Ren, X. & Lu, Z. Visible light promoted difunctionalization reactions of alkynes. *Chin. J. Catal.* **40**, 1003–1019 (2019).

39. Hu, C., Mena, J. & Alabugin, I. V. Design principles of the use of alkynes in radical cascades. *Nat. Rev. Chem.* **7**, 405–423 (2023).

40. Zhang, Y., Cai, Z., Warratz, S., Ma, C. & Ackermann, L. Recent advances in electrooxidative radical transformations of alkynes. *Sci. China Chem.* **66**, 703–724 (2023).

41. Liu, W. & Kong, W. Ni-catalyzed stereoselective difunctionalization of alkynes. *Org. Chem. Front.* **7**, 3941–3955 (2020).

42. Ghosh, S., Chakrabortty, R. & Ganesh, V. Dual functionalization of alkynes utilizing the redox characteristics of transition metal catalysts. *ChemCatChem* **13**, 4262–4298 (2021).

43. Zhu, S., Zhao, X., Li, H. & Chu, L. Catalytic Three-component dicarbofunctionalization reactions involving radical capture by nickel. *Chem. Soc. Rev.* **50**, 10836–10856 (2021).

44. Xu, L., Wang, F., Chen, F., Zhu, S. & Chu, L. Recent advances in photoredox/nickel dual-catalyzed difunctionalization of alkenes and alkynes. *Chin. J. Org. Chem.* **42**, 1–15 (2022).

45. Cui, X. et al. Enantioselective cyclopropenation of alkynes with acceptor/acceptor-substituted diazo reagents via Co(II)-based metalloradical catalysis. *J. Am. Chem. Soc.* **133**, 3304–3307 (2011).

46. Zhang, C., Wang, D.-S., Lee, W.-C. C., McKillop, A. M. & Zhang, X. P. Controlling enantioselectivity and diastereoselectivity in radical cascade cyclization for construction of bicyclic structures. *J. Am. Chem. Soc.* **143**, 11130–11140 (2021).

47. Zhang, H., Chen, B. & Zhang, G. Enantioselective 1,2-alkylhydroxylmethylation of alkynes via chromium/cobalt cocatalysis. *Org. Lett.* **22**, 656–660 (2020).

48. Li, Q.-Z., Li, Z.-H., Kang, J.-C., Ding, T.-M. & Zhang, S.-Y. Ni-catalyzed, enantioselective three-component radical relayed reductive coupling of alkynes: synthesis of axially chiral styrenes. *Chem Catal.* **2**, 3185–3195 (2022).

49. Gu, Q.-S., Li, Z.-L. & Liu, X.-Y. Copper(I)-catalyzed asymmetric reactions involving radicals. *Acc. Chem. Res.* **53**, 170–181 (2020).

50. Dong, X.-Y., Li, Z.-L., Gu, Q.-S. & Liu, X.-Y. Ligand development for copper-catalyzed enantioconvergent radical cross-coupling of racemic alkyl halides. *J. Am. Chem. Soc.* **144**, 17319–17329 (2022).

51. Lin, J.-S. et al. A dual-catalytic strategy to direct asymmetric radical aminotrifluoromethylation of alkenes. *J. Am. Chem. Soc.* **138**, 9357–9360 (2016).

52. Dong, X.-Y. et al. A general asymmetric copper-catalysed sonogashira C(sp^3)–C(sp) coupling. *Nat. Chem.* **11**, 1158–1166 (2019).

53. Cheng, Y.-F. et al. Cu-catalysed enantioselective radical heteroatomic S–O cross-coupling. *Nat. Chem.* **15**, 395–404 (2023).

54. Chen, J.-J. et al. Enantioconvergent Cu-catalyzed N-alkylation of aliphatic amines. *Nature*, DOI: 10.1038/s41586-41023-05950-41588 (2023).

55. Wang, F.-L. et al. Mechanism-based ligand design for copper-catalysed enantioconvergent C(sp^3)–C(sp) cross-coupling of tertiary electrophiles with alkynes. *Nat. Chem.* **14**, 949–957 (2022).

56. Cheng, J. K., Xiang, S.-H., Li, S., Ye, L. & Tan, B. Recent advances in catalytic asymmetric construction of atropisomers. *Chem. Rev.* **121**, 4805–4902 (2021).

57. Cheng, J. K., Xiang, S.-H. & Tan, B. Organocatalytic enantioselective synthesis of axially chiral molecules: development of strategies and skeletons. *Acc. Chem. Res.* **55**, 2920–2937 (2022).

58. Bao, X., Rodriguez, J. & Bonne, D. Enantioselective synthesis of atropisomers with multiple stereogenic axes. *Angew. Chem., Int. Ed.* **59**, 12623–12634 (2020).

59. Mei, G.-J., Koay, W. L., Guan, C.-Y. & Lu, Y. Atropisomers beyond the C–C axial chirality: advances in catalytic asymmetric synthesis. *Chem* **8**, 1855–1893 (2022).

60. Zhang, H.-H. & Shi, F. Organocatalytic atroposelective synthesis of indole derivatives bearing axial chirality: strategies and applications. *Acc. Chem. Res.* **55**, 2562–2580 (2022).

61. Zhang, Z.-X., Zhai, T.-Y. & Ye, L.-W. Synthesis of axially chiral compounds through catalytic asymmetric reactions of alkynes. *Chem Catal.* **1**, 1378–1412 (2021).

62. Qin, W., Liu, Y. & Yan, H. Enantioselective synthesis of atropisomers via vinylidene *ortho*-quinone methides (VQMs). *Acc. Chem. Res.* **55**, 2780–2795 (2022).

63. Feng, J. & Gu, Z. Atropisomerism in styrene: synthesis, stability, and applications. *SynOpen* **5**, 68–85 (2021).

64. Wu, S., Xiang, S.-H., Cheng, J. K. & Tan, B. Axially chiral alkenes: atroposelective synthesis and applications. *Tetrahedron Chem* **1**, 100009 (2022).

65. Zheng, S.-C. et al. Organocatalytic atroposelective synthesis of axially chiral styrenes. *Nat. Commun.* **8**, 15238 (2017).

66. Jia, S. et al. Organocatalytic enantioselective construction of axially chiral sulfone-containing styrenes. *J. Am. Chem. Soc.* **140**, 7056–7060 (2018).

67. Wang, Y.-B. et al. Rational design, enantioselective synthesis and catalytic applications of axially chiral EBINOLs. *Nat. Catal.* **2**, 504–513 (2019).

68. Jin, L. et al. Atroposelective synthesis of axially chiral styrenes via an asymmetric C–H functionalization strategy. *Chem* **6**, 497–511 (2020).

69. Wang, J. et al. Tandem iridium catalysis as a general strategy for atroposelective construction of axially chiral styrenes. *J. Am. Chem. Soc.* **143**, 10686–10694 (2021).

70. Wu, S. et al. Urea group-directed organocatalytic asymmetric versatile dihalogenation of alkenes and alkynes. *Nat. Catal.* **4**, 692–702 (2021).

71. Ji, D. et al. Palladium-catalyzed asymmetric hydrophosphination of internal alkynes: atroposelective access to phosphine-functionalized olefins. *Chem* **8**, 3346–3362 (2022).

72. Yokose, D., Nagashima, Y., Kinoshita, S., Nogami, J. & Tanaka, K. Enantioselective synthesis of axially chiral styrene-carboxylic esters by rhodium-catalyzed chelation-controlled [2+2+2] cycloaddition. *Angew. Chem., Int. Ed.* **61**, e202202542 (2022).

73. Liu, M. et al. Pd^{II}-catalyzed C(alkenyl)−H activation facilitated by a transient directing group. *Angew. Chem., Int. Ed.* **61**, e202203624 (2022).

74. Yan, J.-L. et al. Carbene-catalyzed atroposelective synthesis of axially chiral styrenes. *Nat. Commun.* **13**, 84 (2022).

75. Li, W. et al. Synthesis of axially chiral alkenylboronates through combined copper- and palladium-catalysed atroposelective arylboration of alkynes. *Nat. Synth.* **2**, 140–151 (2023).

76. Sheng, F.-T. et al. Control of axial chirality through NiH-catalyzed atroposelective hydrofunctionalization of alkynes. *ACS Catal.* **13**, 3841–3846 (2023).

77. Feng, J., Li, B., He, Y. & Gu, Z. Enantioselective synthesis of atropisomeric vinyl arene compounds by palladium catalysis: a carbene strategy. *Angew. Chem., Int. Ed.* **55**, 2186–2190 (2016).

78. Jolliffe, J. D., Armstrong, R. J. & Smith, M. D. Catalytic enantioselective synthesis of atropisomeric biaryls by a cation-directed *O*-alkylation. *Nat. Chem.* **9**, 558–562 (2017).

79. Liang, D., Xiao, W., Lakhdar, S. & Chen, J. Construction of axially chiral compounds *via* catalytic asymmetric radical reaction. *Green Synth. Catal.* **3**, 212–218 (2022).

80. Zhang, C. et al. Access to axially chiral styrenes *via* a photoinduced asymmetric radical reaction involving a sulfur dioxide insertion. *Chem Catal.* **2**, 164–177 (2022).

81. Wang, X., Ding, Q., Yang, C., Yang, J. & Wu, J. Enantioselective sulfonylation using sodium hydrogen sulfite, 4-substituted hantzsch esters and 1-(arylethynyl)naphthalen-2-ols. *Org. Chem. Front.* **10**, 92–98 (2023).

82. Lin, Z., Hu, W., Zhang, L. & Wang, C. Nickel-catalyzed asymmetric cross-electrophile *trans*-aryl-benzylation of *α*-naphthyl propargylic alcohols. *ACS Catal.*, 6795–6803 (2023).

83. Amiel, Y. The thermal and the copper-catalyzed addition of sulfonyl bromides to phenylacetylene. *J. Org. Chem.* **39**, 3867–3870 (1974).

84. Lucas, E. L. & Jarvo, E. R. Stereospecific and stereoconvergent cross-couplings between alkyl electrophiles. *Nat. Rev. Chem.* **1**, 0065 (2017).

85. Zhang, X. & Tan, C.-H. Stereospecific and stereoconvergent nucleophilic substitution reactions at tertiary carbon centers. *Chem* **7**, 1451–1486 (2021).

86. Marchese, A. D., Adrianov, T. & Lautens, M. Recent strategies for carbon−halogen bond formation using nickel. *Angew. Chem., Int. Ed.* **60**, 16750–16762 (2021).

87. Paik, A. et al. Recent advances in first-row transition-metal-mediated C−H halogenation of (hetero)arenes and alkanes. *Asian J. Org. Chem.* **11**, e202200060 (2022).

88. Zhang, W., Xu, H., Xu, H. & Tang, W. DABCO-catalyzed 1,4-bromolactonization of conjugated enynes: highly stereoselective formation of a stereogenic center and an axially chiral allene. *J. Am. Chem. Soc.* **131**, 3832–3833 (2009).

89. Zhang, W. et al. Enantioselective bromolactonization of conjugated (*Z*)-enynes. *J. Am. Chem. Soc.* **132**, 3664–3665 (2010).

90. Li, H., Müller, D., Guénée, L. & Alexakis, A. Copper-catalyzed enantioselective synthesis of axially chiral allenes. *Org. Lett.* **14**, 5880–5883 (2012).

91. Li, H., Grassi, D., Guénée, L., Bürgi, T. & Alexakis, A. Copper-catalyzed propargylic substitution of dichloro substrates: enantioselective synthesis of trisubstituted allenes and formation of propargylic quaternary stereogenic centers. *Chem. - Eur. J.* **20**, 16694–16706 (2014).

92. Ng, J. S. & Hayashi, T. Asymmetric synthesis of fluorinated allenes by rhodium-catalyzed enantioselective alkylation/defluorination of propargyl difluorides with alkylzincs. *Angew. Chem., Int. Ed.* **60**, 20771–20775 (2021).

93. O'Connor, T. J., Mai, B. K., Nafie, J., Liu, P. & Toste, F. D. Generation of axially chiral fluoroallenes through a copper-catalyzed enantioselective *β*-fluoride elimination. *J. Am. Chem. Soc.* **143**, 13759–13768 (2021).

94. Zhang, Y. & Vessally, E. Direct halosulfonylation of alkynes: an overview. *RSC Adv.* **11**, 33447–33460 (2021).

95. Truce, W. E., Goralski, C. T., Christensen, L. W. & Bavry, R. H. The copper-catalyzed addition of arenesulfonyl chlorides to conjugated dienes, trienes, and phenylacetylene. *J. Org. Chem.* **35**, 4217–4220 (1970).

96. Amiel, Y. Addition of sulfonyl chlorides to acetylenes. *Tetrahedron Lett.* **12**, 661–663 (1971).

97. Telfer, S. G. & Kuroda, R. 1,1′-Binaphthyl-2,2′-diol and 2,2′-diamino-1,1′-binaphthyl: versatile frameworks for chiral ligands in coordination and metallosupramolecular chemistry. *Coord. Chem. Rev.* **242**, 33–46 (2003).

98. Tan, B. (ed.) *Axially Chiral Compounds: Asymmetric Synthesis and Applications* (Wiley, 2021).

99. Yang, W. et al. Enantioselective hydroxylation of dihydrosilanes to si-chiral silanols catalyzed by in situ generated copper(ii) species. *Angew. Chem., Int. Ed.* **61**, e202205743 (2022).

100. Wang, L.-L. et al. A General copper-catalysed enantioconvergent radical Michaelis–Becker-type C(sp^3)–P cross-coupling. *Nat. Synth.* **2**, 430–438 (2023).

101. Zhou, H. et al. Copper-catalyzed chemo- and enantioselective radical 1,2-carbophosphonylation of styrenes. *Angew. Chem., Int. Ed.* **62**, e202218523 (2023).

102. Sladojevich, F., Trabocchi, A., Guarna, A. & Dixon, D. J. A new family of cinchona-derived amino phosphine precatalysts: application to the highly enantio- and diastereoselective silver-catalyzed isocyanoacetate aldol reaction. *J. Am. Chem. Soc.* **133**, 1710–1713 (2011).

103. Schreiner, P. R. Metal-free organocatalysis through explicit hydrogen bonding interactions. *Chem. Soc. Rev.* **32**, 289–296 (2003).

104. Taylor, M. S. & Jacobsen, E. N. Asymmetric catalysis by chiral hydrogen-bond donors. *Angew. Chem., Int. Ed.* **45**, 1520–1543 (2006).

105. Gimeno, M. C. & Herrera, R. P. Hydrogen bonding and internal or external Lewis or Brønsted acid assisted (thio)urea catalysts. *Eur. J. Org. Chem.* **2020**, 1057–1068 (2020).

Data availability

Data relating to the materials and methods, optimization studies, experimental procedures, mechanistic studies, DFT calculations, HPLC spectra, NMR spectra, and mass spectrometry are available in the Supplementary Information. Crystallographic data for compounds **L6**, **L7**, **N1**, **N30** and **O1** are available free of charge from the Cambridge Crystallographic Data Centre under reference numbers CCDC 2259801 (for **L6**), 2259802 (for **L7**), 2259803 (for **N1**), 2259804 (for **N30**) and 2259805 (for **O1**). All other data are available from the authors upon reasonable request.

Acknowledgements

This work is dedicated to Professor Vivian Wing Wah Yam on the occasion of her 60th birthday. Financial support from the National Key R&D Program of China (Nos. 2021YFF0701604 and 2021YFF0701704), National Natural Science Foundation of China (Nos. 22025103, 92256301, 21831002, 22001109, 22271133, and 22001111), Guangdong Innovative Program (No. 2019BT02Y335), Shenzhen Science and Technology Program (Nos. KQTD20210811090112004, JCYJ20200109141001789, and JCYJ20220818100604009), and Shenzhen Higher Education Institution Stable Support Plan (20200925152921001) is gratefully acknowledged. The authors acknowledge the assistance of SUSTech Core Research Facilities. Computational work was supported by Center for Computational Science and Engineering, and the CHEM high-performance supercomputer cluster (CHEM-HPC) of Department of Chemistry, Southern University of Science and Technology.

Author contributions

J.-B.T. and J.-Q.B. designed the experiments and analyzed the data. J.-B.T., J.-Q.B., Y.-F.C., and L.Q. performed the experiments. Z.Z. and P.Y. designed the DFT calculations. Z.Z. performed the DFT calculations. B.T., Q.-S.G., Z.Z., P.Y., and X.-Y.L. wrote the manuscript. Q.-S.G. and X.-Y.L. conceived and supervised the project.